

Analysis of the Influence of Turbulence on the Heat Transfer Between Spherical Particles and Planar Surfaces

Georg Brösigke^{*a}, Alexander Herter^b, Matthias Rädle^b, Jens-Uwe Repke^a

^aTU Berlin; Process Dynamics and Operation; Strasse des 17. Juni 135, 10623 Berlin, Germany

^bHochschule Mannheim; Department Process Measurement and Innovative Energy Systems; John-Deere-Straße 81a, 68163 Mannheim, Germany
georg.broesigke@tu-berlin.de

The heat transfer of particles and walls plays an important role in several industrial processes. Since established models for the description of that heat transfer are often dealing with simplifications for the surrounding gaseous phase this work aims on getting fundamental understanding of the occurring transport phenomena. In this work a high resolved finite volume method is applied carrying out direct numerical simulation of fluid dynamics and heat transfer simultaneously. The influence of turbulence on the heat transfer mechanisms is discussed in this paper.

1. Introduction

The heat transfer between spherical particles and walls on the one hand and between particles solely on the other hand is relevant in several industrial apparatus, which amongst others include fixed bed reactors, fluidized beds, tube dryers and rotary kilns. For example, Feng et al. (2016) presents a three-dimensional mathematical model for the gas solid heat transfer in sinter bed layers. Several macroscopic influence parameters such as height and diameter of the cooling section as well as particle diameter are investigated. (Singh and Ghule, 2016) present a work where the heat transfer in a fluidized bed stripper ash cooler is investigated both numerically and experimentally. The heat transfer coefficient in their numerical Euler-Euler CFD approach is calculated with two different Nusselt correlations.

Nevertheless, the occurring mechanisms are not fully understood jet or rather their different amount of contribution is not quantified satisfactorily. Since both, purposive development and efficient design are very important aspects in process engineering in terms of Process Intensification and Integration (Klemeš and Varbanov, 2013) a fundamental understanding of the occurring mechanisms is crucial.

In a previous work (Brösigke et al., 2014) the heat conduction through the gap of gas between a single spherical particle and a planar surface was identified as dominating mechanism for the laminar regime. The investigation was carried out with CFD simulations and the results were validated against both experimental data and a correlation from literature for a static sphere on a planar surface (Schlünder, 1984).

For calculating the heat transfer often simplified approaches via Nusselt correlations are chosen. Those correlations are often neglecting transport resistances in the solid phase on the one hand and the actual fluid dynamics in the surrounding fluid (i.e. gas or liquid) phase. In order to identify the basic transport mechanisms the generic system is transformed to a system of basic geometries, i.e. sphere and plate.

2. Methods

Since the particles are small (mm scale) an experimental approach would be connected with enormous effort, if possible at all. In order to investigate all occurring phenomena, a 3D finite volume approach is chosen for the simulations in order to resolve both temperature and velocity boundary layers in all involved phases. Being able to generate a spatial resolution even phenomena on micro scale can be depicted with reasonable effort.

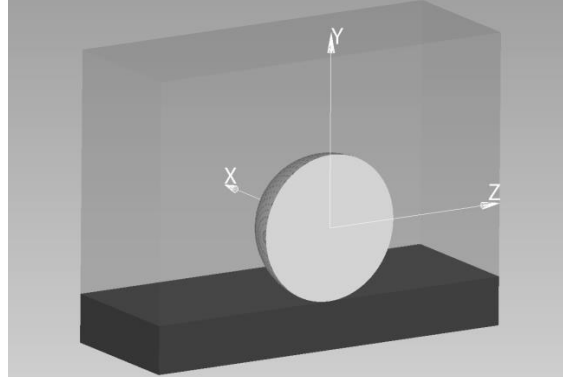


Figure 1: Sketch of CFD Domain with different regions; grey: gas phase; dark grey: plate; bright grey: sphere

2.1 Solver-development

The open source toolbox OpenFOAM® (www.openfoam.org) is used to carry out the simulations. The toolbox offers a variety of preassembled standard solvers, which can be customized in order to meet specific requirements. For the fundamental investigations of the heat transfer between a rolling sphere and plate the solver has to fulfil several requirements, that no standard solver incorporates, i.e. different regions for solid and fluid (gas or liquid), topological mesh movement, temperature dependent physical properties and arbitrary composition of the fluid phase. By modification of the standard solver *chtMultiRegionFoam* with

- the *dynamicFvMesh* library for the topological mesh movement,
- a modified *thermophysicalModels* library for the temperature dependent properties,
- a link between energy and momentum balance, which describes the momentum dissipation,

the postulated requirements can be met.

The simulation domain is built with three different meshes, each representing a region with different physical properties, i.e. sphere, plate and surrounding gas phase. A sketch of the assembly can be seen in Figure 1.

2.2 Simulation conditions

For the fluid phase the compressible Navier-Stokes equations

$$\frac{\partial \rho v}{\partial t} + \nabla(\rho v v) = \nabla(\eta \nabla v) - \nabla p + \rho g \quad (1)$$

are applied, although the Mach Number is small. The reason is to be able to implicitly link density and temperature with the perfect gas equation

$$p v = RT. \quad (2)$$

The heat transfer is described with the energy equation

$$\frac{\partial \rho e + \frac{1}{2} \rho w^2}{\partial t} + \nabla \left(\rho e + \frac{1}{2} \rho w^2 \right) v = \nabla \left(\frac{\lambda}{c_p} \nabla e \right) - \nabla p v + \rho g v + \nabla \tau v \quad (3)$$

incorporating convective and diffusive heat transfer terms as well as the dissipation term. For the solid phase the movement is described by a moving mesh approach and the diffusive heat transport is calculated with the transient heat conduction equation

$$\frac{\partial \rho e}{\partial t} = \nabla \left(\frac{\lambda}{c_p} \nabla e \right). \quad (4)$$

A moved spectator's view is chosen, so that the sphere's mesh performs a rotational movement within the surrounding gas phase. The plate is represented by a mesh adjacent to the bottom of the gas phase. Due to the view of a moved spectator, the plate has to perform a linear movement with the sphere's velocity. The plate's movement is represented by treating the plate as inviscid fluid with the physical properties of a solid, so that the plate's mesh does not have to be moved. The mesh regions are coupled via a Cauchy boundary condition for the temperature and the temperature gradient respectively.

$$T_{sphere,surface} = T_{fluid,surface} \quad (5)$$

$$\dot{q}_{sphere} = \dot{q}_{fluid} \quad (6)$$

By using the arbitrary mesh interface (AMI) mapping function which works with an algorithm using Galerkin projection (Farrell and Maddison, 2011) the faces at the boundaries do not need to be conform.

During the evaluation of the equation system different arithmetic operations have to be carried out including surface and volume integrals next so time integration. In order to do this numerically the operations have to be carried out in discretised form. There exist a variety of suggested discretisation schemes, which have different influence on the solution of the equation system. The upwind differencing scheme increases solution stability due to a numerically dissipative behaviour. It is a first-order scheme which means the interpolation error decreases linear with increasing discretisation resolution. On the other hand, higher order schemes, like central differencing schemes, behave in the opposite way. In Table 1 the applied discretisation schemes are listed for the gas region and the plate region. The significant difference lies in the scheme for the divergence discretisation. For the gas region a scheme of high order, which is not diffusive is applied in order to use the truncation error for turbulence creation. In contrast a 1st order scheme, which is very diffusive is applied for the plate region in order to suppress any turbulence, since this region actually describes a solid.

Table 1: Spatial and temporal discretization schemes for gas and plate region

region	Temporal	gradient	divergence	Laplace
gas	Crank-Nicolson, 2 nd order	least squares, 2 nd order	central differencing, 4 th order	central differencing, 2 nd order
plate	Crank-Nicolson, 2 nd order	central differencing, 2 nd order	upwind, 1 st order	central differencing, 2 nd order

2.3 Meshing

As mentioned in Section 2.1 the three different regions (i.e. sphere, gas and plate) are each treated with an own mesh. The meshes for sphere and plate are physically describing solids, where only the heat flux is investigated in this work, so that the resolution is rather coarse compared to the gas region and the mesh generation is not described in detail. In latter region the fluid dynamics is of high interest, so that the mesh generation is crucial. The mesh for the Direct Numerical Simulation in this region has to fulfil certain conditions. The spatial resolution has to be high in order to resolve all vortices down to where the energy is dissipated, the so called Kolmogorov scale (Ferziger and Peric, 2002).

The mesh is built on the basis of a structured hexahedral mesh which is advantageous for a parallelization during the actual calculation. The sphere is inserted via the OpenFOAM® meshing tool snappyHexMesh. The grid is simultaneously refined in this step. Figure 2 depicts the refined mesh assembly for all regions. The overall domain includes a very high resolved region of interest, which was gained by previous turbulence modelling simulations.

The contact point between sphere and plate cannot be represented in a finite volume method. In the literature several approaches can be found introducing solutions for this task. The particle is flattened near to the contact point to leave a gap between two solid surfaces in the “Caps” approach by Eppinger et al. (2011). Dixon et al. (2013) alternatively give an overview of possible solutions i.e. shrinking, overlap, bridge connection and an approach similar to the Caps approach.

Since this work aims on the fundamental investigation of the heat transfer mechanisms the characteristic geometry of the sphere should be conserved. The contact point is therefore replaced by a gap of 1 µm width, which is resolved with at least four finite volume cells.

2.4 Boundary conditions

The flow fields of gas and plate are velocity driven, since the pressure does not significantly change in this case. Constant values for velocity (5 m/s) and temperature (430 K) are applied at the inlet. At the outlet and the top of the gas phase region a mixed boundary condition is applied, which changes between Dirichlet and Neumann condition depending on the flux's direction. Hereby possible backflow into the domain can be handled. At the boundaries between gas and solid regions the velocity is fixed as well in order to represent the no slip condition for the mentioned moved spectator's view. As mentioned in Section 2.2 as well, a Cauchy boundary condition for the temperature at the contact surfaces of gas and solid is implemented.

The velocity and pressure field results from the turbulence modelling simulations mentioned in Section 2.3 were used as starting guesses for the Direct Numerical Simulations in order to improve convergence. The starting values for the temperature are 550 K for the sphere and 430 K for gas and plate region.

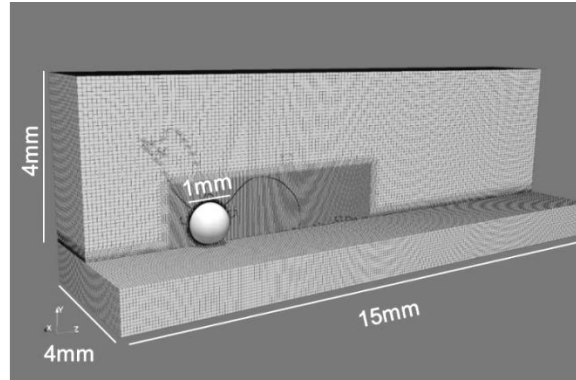


Figure 2: Sketch of the refined mesh assembly

3. Results

Simulations with Reynolds Averaged Navier-Stokes turbulence were carried out for the generation of starting values for the actual Direct Numerical Simulation. In these steady state simulations only the fluid dynamics in the gas phase was solved, neglecting the instationary heat transfer. The OpenFOAM® standard solver simpleFOAM was used and both standard $k-\epsilon$ - and $k-\omega$ -SST-model were applied in a low-Reynolds approach with abstinence of wall functions. Since the standard $k-\epsilon$ -model showed better stability in the convergence behaviour, the DNS was initialized with its results for velocity and pressure field.

The velocity magnitude field for both, DNS and standard $k-\epsilon$ -model are depicted in Figure 3. The domain's symmetry plane in rolling direction is shown, so that the sphere moves from right to left. For the transient DNS a time averaged velocity field is generated for comparison with the stationary RANS model. The simulations show qualitatively similar results with a slight difference in the description of the flow detachment. The Direct Numerical Simulation predicts a more distinct vortex in the flow detachment area behind the sphere and a slightly different shape of the area near the wall.

In Figure 4 the dissipation rate is shown for the same cases shown before. Both results show qualitatively good agreement. Contrary to that the quantity of the dissipated energy differs significantly. The DNS delivers much higher dissipation rates compared to the standard $k-\epsilon$ -model.

In order to determine the influence of turbulence on the heat transfer both convective and diffusive heat flux are calculated and shown in Figure 5 for turbulent conditions (DNS, 5 m/s) on the left hand side and for a simulation under laminar conditions (0.1 m/s) on the right hand side. In each picture the convective heat flux is on the sphere's left hand side and the diffusive heat flux on its right hand side respectively. The sphere rolls towards the observer. Both vector fields are scaled in size with the absolute amount of the heat flux. In colour the heat flux component in Y-direction (i.e. normal to the plate) is represented. Due to the no slip condition on the sphere's surface heat is convectively transported to the plate on the sphere's front side and transported away on the back side. On the other side heat is transported diffusively by conduction normal to the plate. In the turbulent case the both mechanisms take place at the same order of magnitude, whereas in the laminar case the diffusive transport clearly dominates. In Table 2 the overall heat transfer coefficients for the wall heat transfer (k_{wall}) and the heat transfer towards the surrounding fluid (k_{gas}) are listed. The heat transfer for the wall heat transfer is not change significantly affected by the occurrence of turbulence, whereas the heat transfer towards the surrounding fluid increases.

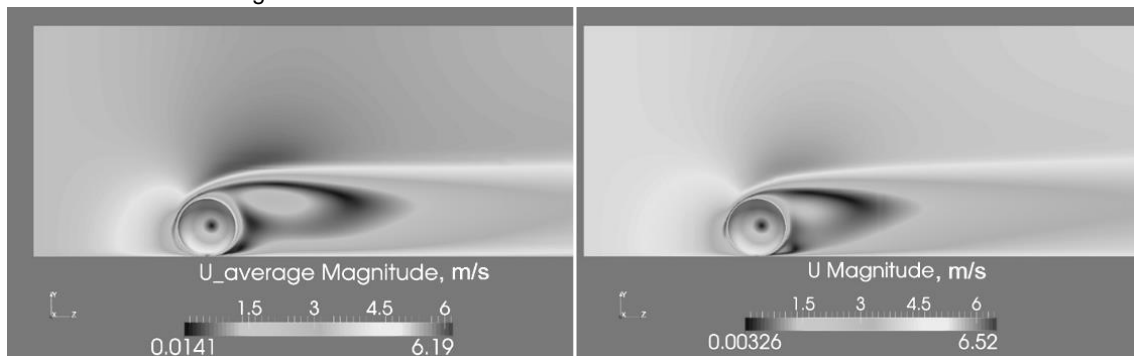


Figure 3: Velocity magnitude fields left: DNS, right: standard $k-\epsilon$ -model

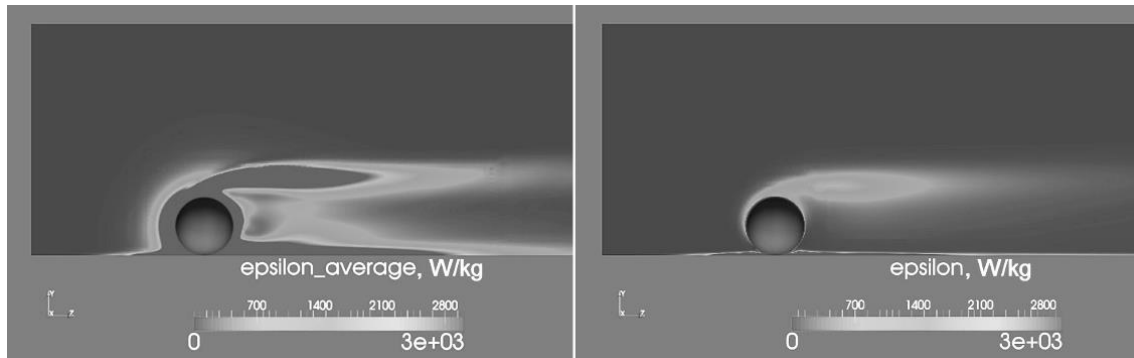


Figure 4. Velocity magnitude fields left: DNS, right: standard k - ϵ -model

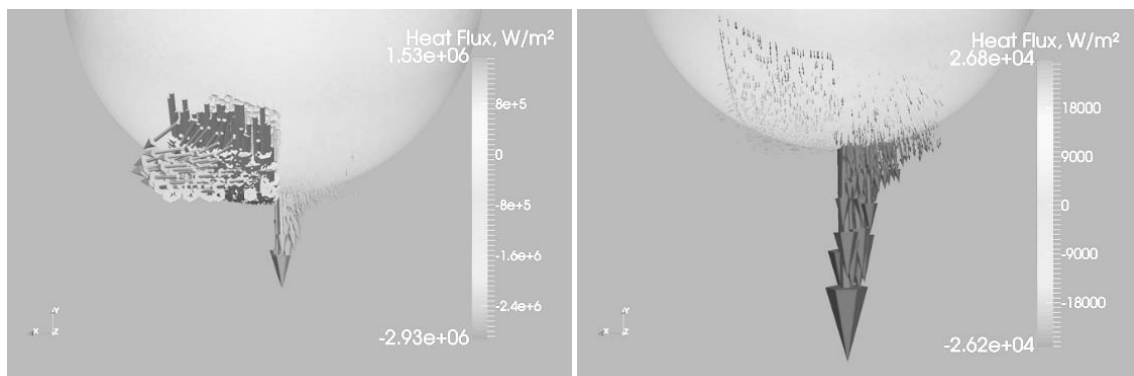


Figure 5. Convective and diffusive heat flux left: DNS, right: laminar

Table 2: Overall heat transfer coefficients

regime	k_{wall} , W/m ² K	k_{gas} , W/m ² K
turbulent	790	437
laminar	807	317

4. Summary and Conclusion

In this paper a first Direct Numerical Simulation of a rolling sphere on a flat plate incorporating the heat transfer is shown. The fluid dynamics is compared against a stationary RANS simulation with the standard k - ϵ -model. It is shown that the turbulence model underestimates the dissipation of turbulent kinetic energy in comparison to the solution of the DNS.

In a second step the result for the heat transfer is compared against a simulation of the heat transfer under laminar conditions. Although the convective heat flux is shown to have increased with the presence of turbulence the overall wall heat transfer coefficient does not change significantly from laminar to turbulent regime. Nevertheless the heat transfer from sphere to the surrounding gas phase increases with rolling speed and occurring turbulence as expected due to the decreased thickness of the boundary layer.

5. Outlook

The thesis that the presence of turbulence seems to have negligible influence on the heat transfer between a rolling sphere and a plate has to be verified by a wider range of parameter variation (e.g. velocity, diameter). For this aim further simulations with turbulence models are planned. It has to be found out if the standard k - ϵ -model's parameters can be calibrated with the result from the DNS in order to represent the correct velocity field and amount of dissipated energy.

Acknowledgments

The authors gratefully acknowledge the financial support of the AIF project GmbH and the Federal Ministry for Economic Affairs and Energy of Germany (Project Number KF 2430009CL2).

References

- Brösigke G., Herter A., Rädle M., Repke J.-U., 2014, Investigations of Heat Transfer Mechanisms between a Moving Sphere and a Static Plate with Computational Fluid Dynamics, 17th Conference on Process Integration, Modelling and Optimisation for Energy Saving and Pollution Reduction, Prague, Czech Republic, Paper ID: 50.
- Dixon A.G., Nijemeisland M., Stitt E.H., 2013, Systematic mesh development for 3D CFD simulation of fixed beds: Contact points study, *Computers & Chemical Engineering*, 48, 135–153
- Eppinger T., Seidler K., Kraume M., 2011, DEM-CFD simulations of fixed bed reactors with small tube to particle diameter ratios. *Chemical Engineering Journal*, 166, 324–331
- Farrell P.E., Maddison J.R., 2011, Conservative interpolation between volume meshes by local Galerkin projection, *Computer Methods in Applied Mechanics and Engineering*, 200, 89–100
- Feng J., Dong H., Gao J., Li H., Liu J., 2016, Numerical investigation of gas-solid heat transfer process in vertical tank for sinter waste heat recovery, *Applied Thermal Engineering*, 107, 135–143
- Ferziger J.H., Perić M., 2002, *Computational Methods for Fluid Dynamics*, Springer Berlin Heidelberg, Berlin, Heidelberg
- Klemeš J.J., Varbanov P.S., 2013, Process Intensification and Integration, *Clean Technologies and Environmental Policy*, 15, 417–422
- OpenFOAM (Open Field Operation and Manipulation), 2011, <www.openfoam.org> accessed 15.04.2016
- Schlünder E.-U., 1984, Heat transfer to packed and stirred beds from the surface of immersed bodies, *Chemical Engineering and Processing*, 18, 31-53
- Singh R.I., Ghule K., 2016, Design, development, experimental and CFD analysis of a prototype fluidized bed stripper ash cooler, *Applied Thermal Engineering*, 107, 1077–1090